Main Manuscript for

A conserved hub protein for coordinating peptidoglycan turnover that activates cell division amidases in *Acinetobacter baumannii*

Brent W. Simpson[a,*], Amanda B. McLean[a], and M. Stephen Trent[a,b,*].

[a]Department of Infectious Diseases, College of Veterinary Medicine, University of Georgia, Athens, Georgia, 30602. USA. [b]Department of Microbiology, College of Art and Sciences; University of Georgia, Athens, Georgia, 30602. USA.

***Email:** strent@uga.edu, bs60907@uga.edu

Author Contributions: B.W.S. designed and performed research, analyzed data, and wrote the manuscript. A.B.M. performed research and analyzed data. M.S.T. designed research, analyzed data, and wrote the manuscript.

Competing Interest Statement: Not applicable.

Classification: BIOLOGICAL SCIENCES. Microbiology.

Keywords: *Acinetobacter baumannii*, cell wall, peptidoglycan, amidase activator, β-lactamase

This PDF file includes:

Main Text
Figures 1 to 7
Figures S1 to S7
Table S1

Abstract

Gram-negative bacteria produce a multilayered cell envelope in which their peptidoglycan is sandwiched between two membranes, an inner membrane made of glycerophospholipids and an asymmetric outer membrane with glycerophospholipids in the inner leaflet and lipopolysaccharide (LPS) in the outer leaflet. The *Acinetobacter baumannii* outer membrane contains lipooligosaccharide (LOS), a variant of LPS lacking O-antigen. LPS/LOS is typically essential, but *A. baumannii* can survive without LOS. Previously, we found that the peptidoglycan biogenesis protein NlpD becomes essential during LOS-deficiency. NlpD is typically redundant and is one of the cell's amidase activators for regulating peptidoglycan degradation, a process critical for cell division. We found that NlpD is essential under these conditions because a second putative amidase activator, termed WthA (cell wall turnover hub protein A), no longer functions in LOS-deficient cells. Mutants lacking WthA had severe cell division defects and were synthetically sick with loss of NlpD. Both *Acinetobacter* WthA and NlpD were found to activate an amidase activity of Oxa51, a chromosomally encoded β-lactamase. Further, WthA is homologous to *Pseudomonas* LbcA that impacts two other classes of peptidoglycan degradation enzymes, endopeptidases and lytic transglycosylases. WthA/LbcA homologs were identified across Proteobacteria, Bacteroidota, and Chlorobiota, suggesting they belong to a conserved family involved in regulation of peptidoglycan turnover. While *Acinetobacter* WthA may share functions of *Pseudomonas* LbcA, we found no evidence that LbcA is an amidase activator. Altogether, we have identified a missing player in *Acinetobacter* peptidoglycan biogenesis, a conserved hub protein that regulates multiple peptidoglycan turnover enzymes including cell division amidases.

Significance Statement

Peptidoglycan is a rigid layer that provides structural support to bacterial cells. Peptidoglycan must be degraded to make room for new synthesis and for cells to divide, a process termed turnover. Turnover enzymes are tightly regulated to prevent their activities from lysing the cell. The critical pathogen *Acinetobacter baumannii* was missing known peptidoglycan amidases, a class of turnover enzymes, and the key activator that controls their activity during cell division. We have identified WthA as having a role in cell division most likely as an amidase activator. WthA homologs were widely distributed in bacteria and the closely related LbcA in *Pseudomonas* impacts two other types of turnover enzymes. We explore the possible functions of this new family of proteins that serves as a hub for impacting peptidoglycan turnover.

Main Text

Introduction

Acinetobacter baumannii is a Gram-negative, opportunistic pathogen with a high incidence of multi- and extreme-drug resistance (1–3). Gram-negative bacteria are naturally resistant to many antimicrobials due to the properties of their dual-membrane cell envelope. Glycerophospholipids make up the inner membrane (IM) that surrounds the cytoplasm. The outer membrane (OM) encloses the IM, periplasm, and cell wall peptidoglycan (PG) layer. Glycerophospholipids are found in the inner leaflet of the OM and glycolipids in the outer leaflet, either lipooligosaccharide (LOS) or lipopolysaccharide (LPS) (4, 5). LOS and LPS both contain a core oligosaccharide attached to a negatively charged lipid A anchor, but LPS also contains a repeated O-antigen polysaccharide (6). The unique amphipathic properties of LOS/LPS packed tightly on the surface of the OM makes it highly impermeable to a wide range of molecules (7). In addition to serving a barrier role in the OM, LOS/LPS also provides structural rigidity to the OM and is essential in most Gram negatives (8–11).

Cationic antimicrobial peptides, including polymyxins, have taken advantage of the conserved negative charge of LPS/LOS to bind and disrupt the OM (12). Polymyxins are used as last-resort antibiotics to treat multi-drug resistant Gram-negative infections, but unfortunately have nephrotoxic side effects (13, 14). *A. baumannii* naturally produces LOS in its OM, but in response

to high levels of polymyxins can obtain mutations to completely abolish LOS synthesis (15, 16). This represents an extreme transformation of the OM to promote antibiotic resistance. While a few other bacteria can survive with inactivation of LPS/LOS synthesis (17–19), *A. baumannii* is the only one that has been observed to do so as a mechanism of drug resistance (15). The complete absence of LOS in the OM has many trade-offs including a poor growth rate, sensitivity to antibiotics normally blocked by LOS, and stress in maintaining the cell envelope (11, 15, 16, 20–22).

The ability of *A. baumannii* to live in the absence of LOS, provides a unique tool to explore novel mechanisms of cell envelope biology and *Acinetobacter* physiology. We previously performed saturated transposon (Tn) mutagenesis in both cells with and without LOS, and used high-throughput, next generation sequencing (Tn-seq) to identify all genes disruptions with increased or decreased fitness (11). A large category of genes that impacted fitness of LOS-deficient cells were genes involved in growth, maintenance, and division of the PG cell wall. PG is a rigid mesh with chains of alternating GlcNAc and MurNAc sugars (*N*-acetylglucosamine and *N*-acetylmuramic acid, respectively) that are crosslinked by short peptides attached to MurNAc residues (23). PG precursors called lipid II are synthesized in the cytoplasm and are composed of GlcNAc-MurNAc-pentapeptide subunit attached to an undecaprenyl-phosphate lipid carrier (23). Lipid II is flipped across the IM by the flippase, MurJ (24) where PG synthases then polymerize and crosslink PG subunits into the cell wall by glycosyltransferase and transpeptidase activities, respectively (23). Synthesis of the cell wall is highly coordinated with degradation enzymes that make room for newly inserted material and that remodel division sites for daughter cell separation, a process called turnover. PG turnover enzymes are highly regulated to assure that their activity is balanced with synthesis. Here, we explored an apparent cell division defect in LOS-deficient *A. baumannii* involving regulation of PG degradation enzymes.

Several auxiliary genes for cell division (*nlpD, tolA, tolB, tolQ, tolR, pal,* and *yraP*) became critical for fitness in LOS-deficient *A. baumannii* (11). TolABQR and Pal make up the Tol-Pal system. Tol-Pal has been implicated in coordinating cell division PG turnover through NlpD (25), invagination of the OM (26), and impacting transport of glycerophospholipids between the IM and OM (27). YraP is an outer membrane lipoprotein of unknown function that was also suggested to impact PG turnover via NlpD (25). NlpD is a degenerate member of LytM family endopeptidases, a PG turnover family, that is missing catalytic residues to degrade PG itself (28). Instead, NlpD localizes to septa and activates PG amidases (AmiC in *E. coli*) that cleave the amide bond between MurNAc and crosslinked peptides (28, 29). PG amidases completely release the crosslinked peptides and leave a so-called “denuded” sugar polymer. NlpD is usually redundant with additional degenerate LytM-domain proteins that activate amidases, such as EnvC and ActS in *E. coli* (29–31). In most proteobacteria described thus far, EnvC is the primary amidase activator for cell division (**Fig. 1**), but defects in *envC* mutants are exacerbated by loss of NlpD, Tol-Pal, and YraP (25). Because these genes had become critical for fitness in LOS-deficient *A. baumannii*, we suspected that a cell division amidase activator was no longer functioning when the OM was perturbed by absence of LOS. However, *A. baumannii* was missing homologs of *envC* and missing any known amidases. We sought to use the LOS-deficient genetic background to identify genes involved in cell division amidase activation.

Cell division amidases play an important role in a self-enhancing loop to increase division activity (**Fig. 1**). Recruitment of divisome components is highly ordered and reviewed well by others (32, 33). Important here, FtsEX acts upstream to regulate EnvC (23). After the Z-ring and divisome complexes have already formed and started to synthesize septal PG, ATP hydrolysis by FtsEX triggers a conformational change in EnvC so that a self-inhibiting domain releases from the degenerate LytM domain (34–36). EnvC can then activate AmiB or AmiA to cleave peptides from the septal PG. The resulting “denuded” PG is recognized by the SPOR domain of FtsN (37). Conformational changes of FtsN signal both through FtsQLB to activate PBP3 (divisome transpeptidase) and through FtsA to activate FtsW (divisome glycosyltransferase) (38–41). Increased septal PG synthesis by PBP3/FtsW further promotes recruitment of more FtsN leading

to a self-enhancing cycle of septal PG synthesis and processing to drive division to completion (38). *A. baumannii* contains a single, essential homolog of FtsN (42, 43), suggesting that it is still utilizes this cell division reinforcement loop (**Fig. 1**). However, *A. baumannii* is missing FtsEX, EnvC, and AmiABC.

Here, we utilized the cell division defect of LOS-deficient *A. baumannii* to identify a gene (HMPREF0010_01334 in strain ATCC 19606) named here WthA, that impacts cell division and growth. WthA is periplasmic and contains a high number of TPR (tetratricopeptide repeat) domains that facilitate protein-protein interactions. Further, it was redundant with NlpD, suggesting that it activates amidases. Indeed, there is a precedence for TPR domains activating amidases as *Staphylococcus aureus* contains ActH which uses TPR domains to activate a PG amidase (44, 45). Additionally, we demonstrate that both NlpD and WthA induce formation of PG amidase products when co-expressed with the β-lactamase, Oxa51, further cementing this new function as an amidase activator. This finding supports the recent proposal that *A. baumannii* β-lactamases can both degrade β-lactams and cleave PG as amidases (46). Our data supports that *A. baumannii* WthA may regulate multiple PG turnover enzymes and have named it cell wall turnover hub protein A. WthA homologs are widely conserved in Proteobacteria, Bacteroidota and Chlorobiota. LbcA, an ortholog of WthA in *Pseudomonas aeruginosa*, facilitates proteolysis of endopeptidases that cleave PG crosslinks and binds to lytic transglycosylases that cleave the sugar chains of PG (47, 48). However, the existing literature and data presented here indicates that the *Pseudomonas* homolog does not serve as an amidase activator. Overall, our data suggests that WthA/LbcA homologs are a family of hub proteins for regulation of PG turnover enzymes with possibly distinct mechanisms.

Results

HMPREF0010_01334 is involved in cell division and does not function in LOS-deficient cells.

We suspected that an unknown cell division amidase activator was not functioning in LOS-deficient *A. baumannii* based on the following logic. In *E. coli*, loss of NlpD, Tol-Pal, and YraP were synthetic sick with loss of the primary cell division amidase activator EnvC (25, 29). In LOS-deficient *A. baumannii*, NlpD, Tol-Pal, and YraP were found to be critical for fitness (11) (**Fig. S1A)**. *A. baumannii* had no homolog of EnvC, but likely still used a cell division amidase activator because it had an essential FtsN homolog (42, 43) (HMPREF0010_03200) with a SPOR domain for sensing the product of PG amidases, PG glycan chains denuded of crosslinked peptides (**Fig. 1**). Finally, it was unlikely that NlpD served as the primary cell division amidase activator, because it was not essential in LOS-containing *A. baumannii* and its disruption caused only rare chaining (**Fig. S1**). Also in agreement with this logic, LOS-deficient strains had a chaining defect (22) (**Fig. 2A**) and naturally increased expression of NlpD (16), possibly to compensate for reduced function of the other amidase activator. If the missing cell division amidase activator was no longer functioning in LOS-deficient *A. baumannii*, then it may have a positive fold-change in our LOS-deficient Tn-seq. We have seen this type of Tn-seq "signature" for all genes involved in synthesis and transport of LOS; *lpx* and *lpt* genes were easy to disrupt in LOS-deficient cells because they were not functioning (11). HMPREF0010_01334 (renamed here *wthA* for cell wall turnover hub protein A) fit these criteria. Tn-seq showed low RPKMs for transposons in this gene in a strain containing LOS and a positive fold change in our LOS-deficient strain (11) (**Fig. S1A**).

First, we constructed a *wthA* deletion mutant and assessed by microscopy for division defects. *wthA* is in an operon with *lolB* and contains the native *lolB* RBS within the *wthA* open reading frame (ORF). We deleted nucleotides 1-1535 out of the 1638 nucleotide *wthA* ORF to prevent polar effects on *lolB* (**Fig. 2B**). We also constructed an in *cis* complement strain that mimicked this alteration to *lolB*, introduced a new RBS for *lolB*, and left *wthA* intact (**Fig. 2B**). The *wthA* mutant had a severe cell division defect with long, kinked chains of cells, evident lysis, and even rare instance of branched cells at failed division sites (**Fig. 2A**). The in *cis* complement strain had no morphological differences compared to the wild-type parent, suggesting the division defects were not due to polar effects on *lolB* (**Fig. 2A**). To get a closer look at the possible failed division

sites in Δ*wthA*, we performed transmission electron microscopy. The *wthA* mutant notably had a severely detached OM, chains with several division sites, and extension of some of these division sites that gave them the kinked appearance (**Fig. 2C**). Next, we performed growth curves in LB and in a hyperosmotic condition, LB supplemented with 10% glycerol. In LB, the Δ*wthA* mutant had a reduced growth rate compared to the complement and wild-type strains (**Fig. 2D**). In hyperosmotic conditions, the Δ*wthA* mutant failed to grow at all (**Fig. 2E**), suggesting that rigidity of the cell wall had been perturbed. It was evident that loss of WthA was causing lysis during growth in LB because the optical density decreased after ~8-10 hours of growth (**Fig. 2D**) and overnight cultures had accumulation of cellular debris (**Fig. S2**).

To further address if *wthA* phenotypes were due to polar effects on *lolB*, we sought to also complement the mutant in *trans*. The Δ*wthA* mutant was incapable of transformation; repeated attempts and alterations of our transformation protocol resulted in no successful transformants. To increase the transformation efficiency, we built a mutant disrupting the operon of a type II restriction endonuclease (HMPREF0010_00560 and HMPREF0010_00561) (**Fig. S3A**). We named the resulting strain 19606e for electrocompetent and assessed its impact on plasmid transformation. The 19606e strain had ~130-fold increase in transformation efficiency and did not impact growth or cell morphology (**Fig. S3B-D**). We next deleted *wthA* in the 19606e background and successfully transformed in plasmids to test complementation. The *wthA* gene alone or in combination with *lolB* in *trans* were sufficient to complement defects of the 19606e Δ*wthA* mutant (**Fig. 3** and **S2**). The *lolB* plasmid did not complement 19606e Δ*wthA* (**Fig. 3** and **S2**), indicating that the mutant phenotypes were not due to polar effects on *lolB*.

While maintaining the *wthA* mutant in the laboratory, we noted that the mutant showed poor growth after storage of agar plates at 4°C. This was a striking phenotype because it is shared by LOS-deficient strains. To test this, LOS^+ cells lacking *wthA* and wild-type LOS-deficient cells were grown on two separate LB agar plates at 37°C overnight. Wild-type 19606 containing LOS was used as a positive control. For each strain, one plate was stored at room temperature and another stored at 4°C for 7-8 days. Single colonies from each storage condition were restruck on LB agar and incubated at 37°C. Compared to wild-type LOS^+ cells, Δ*wthA* and LOS-deficient mutants exhibited poor growth following storage at 4°C (**Fig. 2F**). This supported that WthA was likely not functioning well in LOS-deficient cells and that reduction of WthA function likely caused the sensitivity to cold storage observed in LOS-deficient strains.

WthA impact on cell division is separate from possible impacts on PG lytic enzymes MepM and MltD.

The phenotypes observed were all consistent with loss of WthA causing a defect in PG biogenesis. Next, we tested for sensitivity to PG-targeting antibiotics to pinpoint what stage of PG synthesis or turnover might be influenced. Loss of *wthA* did not impact sensitivity to fosfomycin (targets MurA) which suggested synthesis of lipid II precursors was unperturbed, nor did it alter sensitivity to bacitracin (targets undecaprenyl-phosphate) which suggested that undecaprenyl recycling was not affected (**Table S1.**). Instead, the *wthA* mutant had both increased resistance to vancomycin (targets D-ala-D-ala) and increased sensitivity to beta-lactams, aztreonam and ceftazidime-avibactam, (target PBPs), which suggested that PBP transpeptidation was low resulting in a build-up of uncrosslinked D-ala-D-ala's (**Table S1**). Since amidases are thought to signal for FtsN activation of the FtsW/PBP3 (**Fig. 1)**, this profile of antibiotic sensitivity was consistent with the possibility that WthA could be a cell division amidase activator. We also observed that the *wthA* mutant was hypersensitive to rifampicin, a drug blocked by LOS in the OM (**Table S1**). This was consistent with the severe alteration of the OM observed in the transmission electron microscopy (**Fig. 2C**).

We then selected for suppressors during growth in hyperosmotic media to further understand the PG defect in *wthA* mutants. The Δ*wthA* mutant was passaged in LB with increasing

concentrations of glycerol. After passaging from LB with 5% glycerol to media with 10% glycerol, two cultures had recovered growth and were subjected to whole-genome sequencing. Population one contained a frameshift, *mepM(G156fs)*, that would disrupt the endopeptidase, MepM, and population two contained a frameshift, *mltD(V307fs)*, that would disrupt the lytic transglycosylase, MltD (**Fig. 4A**). The ortholog of WthA found in *P. aeruginosa*, named LbcA, binds to both MepM and MltD (47, 48) (**Fig. 4B**). LbcA serves as an adaptor to direct three different endopeptidases (MepM, PA1198, PA1199) to the protease CtpA (47, 48). LbcA was also found to bind the lytic transglycosylases, MltD and RlpA, although neither were protease substrates and these interactions may be indirect through additional protein partners (48). The suppressors suggested that the mechanism by which WthA and LbcA affects MepM and MltD function were likely conserved (**Fig. 4B-C)**.

We suspected that impacts on MepM and MltD were not responsible for cell division defects upon loss of WthA, because these functions would be shared by LbcA and it has been well documented that *Pseudomonas lbcA* mutants showed no growth or cell division defects (**Fig. 4D)** (47). Instead, disruption of PG lytic enzymes could be beneficial to Δ*wthA* if PG synthesis is low, as suggested by the antibiotic sensitivity profile (**Table S1**). This effect has been observed for β-lactam inhibition of PG synthesis, during which lysis is attributed to PG degradation still being high while synthesis is low (29, 49–52). To dissect how MepM and MltD disruptions rescued the Δ*wthA* mutant, we deleted each gene in combination with Δ*wthA*. *mepM* and *mltD* single mutants had no growth defect in LB or LB with 10% glycerol (**Fig. S4**). When combined with Δ*wthA*, the Δ*mepM* Δ*wthA* and Δ*mltD* Δ*wthA* double mutants partially rescued growth on LB with 10% glycerol and fully rescued growth on LB (**Fig. 4E-F**). However, the engineered suppressors, Δ*mepM* Δ*wthA* and Δ*mltD* Δ*wthA*, still had cell division defects, including chaining and morphology defects in divided cells (**Fig. 4G**). This suggested that the suppressors reduced PG degradation to match with PG synthesis being low. It also suggested that WthA's possible impacts on MepM and MltD function were not responsible for the cell division defects. Notably, *P. aeruginosa* utilize EnvC as the primary amidase activator for cell division (53), whereas *A. baumannii* are missing EnvC and may utilize WthA instead (**Fig. 4B-C**).

WthA and NlpD alterations have synthetic effects, suggesting partial redundancy.

We suspected that NlpD was critical for fitness in LOS-deficient cells because WthA was not functioning. Since part of the cellular response during LOS-deficiency was to increase expression of NlpD (16), we first tested if NlpD overexpression was beneficial to *wthA* mutants. Overexpression of NlpD from an IPTG-inducible plasmid slightly rescued the growth defect of the Δ*wthA* mutant but did not fix cell chaining or morphology (**Fig. 5A-B**). This supported that NlpD and WthA may be partially redundant as amidase activators.

To directly test if loss of NlpD was synthetic sick with loss of WthA, we deleted *nlpD* in a *wthA* depletion strain where expression of *wthA* is under control of an anhydro-tetracycline (aTc)-inducible promoter. We also combined Δ*tolA* with the *wthA* depletion allele to assess another pathway that impacts NlpD function. Depletion of *wthA* alone (no aTc) resulted in a growth defect and slight cellular chaining but was not quite as severe as observed in the deletion mutants (**Fig. 5C-D**). Deletion of *nlpD* or *tolA* combined with *wthA* depletion resulted in a severe exacerbation of the chaining defect, although growth was only slightly further perturbed (**Fig. 5C-D**). E-test (Epsilometer test) assessment of antibiotic sensitivity confirmed that the *wthA* depletion strain did not have as severe of sensitivities to rifampicin, aztreonam, and ceftazidime-avibactam as compared to the *wthA* deletion mutant (**Fig. 5E**). However, combining Δ*nlpD* or Δ*tolA* with the *wthA* depletion allele increased antibiotic sensitivities to levels very similar to the Δ*wthA* mutant (**Fig. 5E**).

Together, these phenotypes indicated that loss of NlpD or Tol-Pal was synthetic sick with depletion of WthA and supported that WthA could be an amidase activator redundant with NlpD.

WthA and NlpD stimulate a toxic amidase activity when co-expressed with beta-lactamase Oxa51.

A. baumannii is missing any homologs of known amidases but have the well-known amidase activator NlpD. This suggests that *A. baumannii* utilizes a different family of amidases. Recently, it was observed that overexpression of a class D serine β-lactamase, Oxa23, caused physiological changes in *A. baumannii* (46). In addition, Oxa23 overexpression increased amidase products in the cell, chains of PG denuded of crosslinked peptides (46). Oxa23 is a plasmid encoded β-lactamase of the *A. baumannii* AB5075 strain. However, all *A. baumannii* strains have several chromosomally encoded β-lactamases suggesting that they could have physiological roles, perhaps as amidases (46). Serine β-lactamases are distantly related to PG degradation enzymes (endopeptidases and D-ala-D-ala carboxypeptidases that cleave PG peptides) and PBPs (54), suggesting that they could act on the PG peptide. The ATCC 19606 strain has a class A (HMPREF0010_01156/*cblA*), class B (HMPREF0010_03656), class C (HMPREF0010_02318/ *ampC*) and class D (HMPREF0010_00844/*oxa51*) β-lactamase encoded on the chromosome. We wondered if the apparent amidase activity during overexpression of a β-lactamase could be increased by NlpD or WthA. Plasmids were constructed to co-express NlpD or WthA with Oxa51 because it was the most closely related to the previously characterized Oxa23.

We immediately saw evidence that co-expression of NlpD or WthA with Oxa51 was toxic to an *E. coli* cloning strain used to generate the plasmids, as many colonies had to be screened to find plasmids without mutations in the genes of interest. We transformed the plasmids into both a wild-type *E. coli* strain (W3110) and *A. baumannii* to characterize the effects of co-expression of these genes. Co-expression of NlpD/Oxa51 or WthA/Oxa51 was toxic to *E. coli* (**Fig. 6A-B**) and *A. baumannii* (**Fig. S4A-B**) strains, whereas expression of the activators or Oxa51 alone had no toxicity. This suggested that NlpD and WthA may be capable of activating the toxic, uncontrolled degradation of PG by Oxa51.

We recently studied PG recycling in *E. coli* (55, 56) and had mutants where we could test if Oxa51 was cleaving PG peptides due to an amidase activity. PG turnover enzymes can produce either a freed peptide (product of amidases) or peptide still linked to a cyclized anhydro-MurNAc and GlcNAc (product of endopeptidases and lytic transglycosylases) (57). *E. coli* recycles nearly 100% of turnover PG products using specialized transporters that recognizes these different species. MppA/OppBCDF and CadB import freed peptides and AmpG imports sugar-linked peptides (55, 56, 58–60). A Δ*opp* Δ*cadB* mutant will specifically only release freed PG peptides to the growth media but will recycle all sugar-linked PG peptides. Thus, in this genetic background released PG peptides serve as a direct proxy for PG amidase activity. To track released peptides, cells were grown in the presence of tritiated meso-diaminopimelic acid (^{3}H Dap) that efficiently labels PG peptides. After removing excess radiolabel, we then monitored for release of ^{3}H Dap into the growth supernatant (**Fig. 6C**). Plasmids expressing Oxa51 alone, NlpD/Oxa51, or WthA/Oxa51 were induced at sublethal levels (**Fig. S5C-D**) during the experiment to prevent any signal from lysed cells. There was no significant difference in the amount of tritiated amidase products released from Oxa51 expression compared to the empty vector (**Fig. 6D**). However, coexpression of NlpD/Oxa51 or WthA/Oxa51 released ~20% of the cellular tritiated PG in the form of amidase products (**Fig. 6D**). This supported that NlpD and WthA serve as amidase activators. Both likely activate an amidase activity of Oxa51, although follow-up experiments will be needed to determine if this is a direct enzymatic function of Oxa51 or indirect effect of the coexpression. Oxa51 could be one of the missing amidases of *A. baumannii*. Deletion of *oxa51* alone did not cause any striking cell division defects (**Fig. S6**). This was not surprising as amidases tend to be highly redundant in other bacteria, making identification difficult. We are actively exploring if Oxa51 serves as a

redundant cell division amidase possibly with other chromosomally encoded proteins annotated as β-lactamases.

WthA/LbcA homologs are conserved in Gram-negative bacteria

All major cell division amidase activators described till now have utilized dLytM domains, EnvC, DipM of *Caulobacter crescentus*, and NlpD/ActS (29, 30, 61) (**Fig. 7A**). WthA is the first putative cell division amidase activator to instead contain TPR domains. Although *Staphylococcus aureus* utilizes ActH to activate an amidase (**Fig. 7A)**, its cognate amidase cleaves uncrosslinked PG peptides to stimulate PG synthesis in a distinct mechanism that is still being unraveled (44, 45). We wondered if this possible function of WthA was conserved in some Gram-negative bacteria. The database String (62) suggested that *wthA* had synteny with *lolB* that was widespread in gamma- and beta-Proteobacteria as well as Bacteroidota. We searched in these and nearby phylogenetic branches for *wthA* homologs. We identified likely *wthA* homologs in these branches of Gram negatives as well as alpha-Proteobacteria and Chlorobiota (**Fig. 7B**). Excitingly, WthA homologs were found in several species of beta- and gamma-Proteobacteria that were missing EnvC and may utilize WthA instead for activating cell division amidases (**Fig. 7B**). Notably *Bacteroides* species are thought to not contain *lolB* homologs. The identified synteny in Bacteroidota was to an unknown function OM lipoprotein encoding gene that String suggested were *lolB* homologs (**Fig. 7B**). This gene could encode a LolB previously missed due to low sequence similarity [20.61% to *E. coli* LolB by Clustal Omega alignment (63)] or could have a different function. In Bacteroidota, *envC* was also in the *wthA* operon (**Fig. 7B**).

Since *A. baumannii wthA* and *P. aeruginosa lbcA* phenotypes differ, homologs of WthA/LbcA could differ in what types of PG turnover enzymes they help modulate (**Fig. 4A-D**). We wondered if *P. aeruginosa* LbcA could also act as an amidase activator. This activity would have been missed due to its potential redundancy with EnvC and NlpD. We cloned codon-optimized alleles of *P. aeruginosa nlpD* and *lbcA* on to plasmids in combination with known amidase gene, *amiB*, and possible amidase gene, *oxa10*, referred to as *Pa*NlpD, *Pa*LbcA, *Pa*AmiB and *Pa*Oxa10, respectively. We screened combination expressions for toxic effects on *E. coli*. Sole expression of *Pa*AmiB had a slight toxicity in *E. coli* (**Fig. 7C**), which would be expected because *E. coli* NlpD and EnvC work with amidases from this family. In agreement with existing literature that *Pa*NlpD functions with *Pa*AmiB (53), coexpression of these proteins was highly toxic (**Fig. 7C** and **S7**). However, *Pa*NlpD coexpression with *Pa*Oxa10 had no evidence of toxicity (**Fig. 7C**). *Pa*LbcA coexpression with *Pa*AmiB or *Pa*Oxa10 did not enhance toxicity of either protein, suggesting that it is not an activator of either protein (**Fig. 7D** and **S7**). Together, no evidence was observed that LbcA could act as an amidase activator. It is possible that the right amidase partner was not tested and that LbcA could activate amidase activity of *P. aeruginosa* AmiA or a different β-lactamase. However, LbcA protein interactions have been highly explored and AmiB is the only amidase that was an identified interaction partner (48).

Since *Pa*Oxa10 had no evidence of amidase activity capable of activation, we wondered if *A. baumannii* Oxa51 had evolved this new activity. We combined *Pa*NlpD and Oxa51 on a plasmid for coexpression. Oxa51 was toxic to *E. coli* when co-expressed with *Pa*NlpD (**Fig. S7C**), suggesting that there are differences between the β-lactamase homologs that allows *A. baumannii* Oxa51 to act as an amidase and be activated by NlpD from multiple species.

Discussion

We have provided evidence that WthA is likely the missing cell division amidase activator in *A. baumannii*. Mutants lacking WthA grew poorly and had severe cell division defects. This explains why transposon insertions in *wthA* are underrepresented in our LOS-containing transposon mutant libraries (11). For this reason, *wthA* mutants were also missing in other recent Tn-seq approaches to globally identify functions for *A. baumannii* genes (64). In addition, because *wthA* is not fully essential, it has also been missing in recent CRISPRi knockdown libraries that globally targeted essential genes (65, 66). We were uniquely able to make a connection to cell

division for this gene because it was not functioning in LOS-deficient cells which led to it being easier to disrupt in this background. In support of WthA not functioning properly in the absence of LOS, LOS-deficient and *wthA* mutants both display cell division defects and were difficult to culture after storage at 4°C. Why WthA does not function when LOS is missing from the OM remains to be seen. It is possible that WthA has an OM protein partner that does not fold correctly with this alteration to the OM.

Reduced function of WthA in LOS-deficient cells also likely led to NlpD, Tol-Pal, and YraP becoming critical for fitness in this background (11). *wthA* mutants were both partially rescued by NlpD overexpression and had exaggerated cell division defects when *nlpD* was absent, supporting their partial redundancy as amidase activators. Furthermore, both NlpD and WthA were toxic when co-expressed with Oxa51, a chromosomally encoded β-lactamase. This finding further supported the proposal from the Rather group (46) that *A. baumannii* β-lactamases can have dual functions of degrading β-lactams and serving as PG peptide amidases. The closely related Oxa23 enzyme was shown to cause physiological differences when overexpressed consistent with alteration to the cell envelope and increased amidase products in the cell (46). We leveraged mutants in *E. coli* PG recycling that specifically only release PG amidase products (55, 56) to develop an assay for amidase activity. Co-expression of WthA/Oxa51 or NlpD/Oxa51 both resulted in release of PG amidase products, supporting the most likely hypothesis that WthA and NlpD activate an amidase activity of Oxa51. However, since our assays are performed in the context of all cellular proteins, it is possible that the observed increase in amidase activity could be indirect. Further work will be needed to identify additional *A. baumannii* amidases and establish through biochemical assays their direct activation by WthA and NlpD.

We have named WthA as a cell wall turnover hub protein because our evidence suggested it activates amidases and its homology to *P. aeruginosa* LbcA suggests that may also impact endopeptidases and lytic transglycosylases (47, 48). Notably, WthA has a conserved N-terminal adaptor domain that facilitates LbcA interaction with the CtpA protease (67, 68) and *A. baumannii* contains CtpA. We also isolated *wthA* suppressors that disrupted encoding genes for two interaction partners of LbcA, MepM and MltD. MepM is a substrate of LbcA/CtpA-mediated proteolysis and MltD is proposed to indirectly interact with LbcA possibly in a larger protein complex (47, 48). Disruption of either MepM or MltD rescued growth defects of the *wthA* mutant. Altogether, these results support that WthA likely has conservation of the described LbcA function. However, WthA's impact on cell division appears to be separate from LbcA-like activities. *P. aeruginosa* mutants lacking LbcA have high protein levels of three endopeptidases, yet were reported to have no morphological defects (47, 48), indicating that increased endopeptidases is not sufficient to cause cell division defects. In addition, loss of MepM or MltD did not rescue the cell division defects of the Δ*wthA* mutant. Together, this evidence supports that impacts on MepM and MltD do not contribute to the cell division defects of Δ*wthA* mutants.

Homologs of WthA/LbcA are wide-spread across alpha-, beta-, and gamma-Proteobacteria as well as Bacteroidota and Chlorobiota (**Fig. 7B**), suggesting these proteins are widely used to regulate PG turnover. Notably, WthA/LbcA homologs have been implicated to affect the cell envelope in *Brucella melitensis* (69), *Brucella abortus* (70), and *Rhizobium leguminosarum* (71) and could function similar to WthA or LbcA. However, likely not all homologs are capable of activating amidases. We found no evidence that LbcA could activate native *P. aeruginosa* amidases. LbcA was not capable of activating a toxic PG degradation when combined with AmiB or Oxa10. This suggested that LbcA and WthA are distinct in how many PG turnover enzymes they coordinate (see **Fig. 4A-C**). How conserved each of these functions are in other Gram-negatives will be interesting to explore. It is curious that LbcA and WthA differ in cellular localization, OM anchored and periplasmic, respectively. Further, all characterized amidase activators that have a major impact on cell division have been periplasmic, EnvC, DipM, and putatively WthA. While, OM lipoprotein amidase activators, NlpD and ActS, have small impacts on cell division. It is possible that having a major role in cell division requires amidase activators to be soluble periplasmic,

perhaps because the OM lags behind during formation and degradation of septal PG. In support of this idea, all organisms that have WthA/LbcA homologs instead of EnvC have soluble periplasmic homologs perhaps more similar in function to WthA (**Fig. 7B)**. Yet, many organisms that have both EnvC and WthA/LbcA still have soluble periplasmic homologs, so this localization is not exclusive to homologs that are the putative primary cell division amidase activator (**Fig. 7B**). Altogether, we have supported that *A. baumannii* utilizes β-lactamases as PG amidases and have identified a new protein, WthA, that impacts cell division as an amidase activator.

Materials and Methods

Media and growth conditions. All cultures and agar plates were performed with Difco™ Luria-Bertani Broth or Agar, Miller (BD). Where appropriate media was supplemented with glycerol (10 % volume/volume), kanamycin (30 μg/mL), tetracycline (5-10 μg/mL), hygromycin B (250 μg/mL for *A. baumannii* and 100 μg/mL for *E. coli*), carbenicillin (100 μg/mL), and anhydro-tetracycline (10 nM, aTc). Concentrations of isopropyl β-D-1-thiogalactopyranoside (IPTG) are indicated in the experiment.

Strains and plasmids. All strains and plasmids used in this study are listed in Data Set S1. All oligonucleotides used in this study were synthesized by IDT or Eurofins Genomics LLC and are listed in Data Set S1. *A. baumannii* 19606 deletion mutants were built by recombineering as described previously (72). The isogenic parent to 19606 recombineered strain, BWS399, was used as the 19606 "wild-type" for this study (11).

An anhydro-tetracycline inducible mutant was built by the same recombineering methodology, but a hygromycin B resistant plasmid, pMMB67EHhph-RecAb, was used for induction of the RecAb system. Primers with the 125 nt of chromosomal homology were used to amplify from the plasmid pBaM3 which contained an outward facing tet-inducible promoter with an upstream and reverse orientation *tetR* regulator and kanamycin resistance cassette flanked by *frt* sites. The carbenicillin resistant pMMB67EH-Flp plasmid was used for removing *kan* cassettes from chromosomal inducible mutants. For the 19606 *tetR-wthA* strain, first the *frt-kan-frt-tetR-ptet* product (described above using pBaM3 template) was recombineered upstream of *wthA* on plates containing 10 nM aTc. Strains with inducible alleles were maintained with 10 nM aTc at all times. After the *kan* cassette was flipped out, a second *kan* cassette and ribosome binding site was recombineered downstream of *wthA* to give *lolB* a separate promoter and ribosome binding site using the 1334-cis-comp recombineering primers (pKD4 template). *tetR-wthA* was combined with *nlpD* and *tolA* deletions using the same methodology, but starting in 19606rec Δ*nlpD::frt* (pMMB67EHhph-RecAb) and 19606rec Δ*tolA::frt* (pMMB67EHhph-RecAb) strains, respectively.

TaKaRa ExTaq® polymerase or Apex™ Taq RED polymerase were used for PCRs <5 kb for cloning or screening experiments, respectively. PFU Turbo polymerase AD (Agilent) was used for PCRs >5 kb. pMMB67EHhph-RecAb was built by amplifying the backbone of pMMB67EH-RecAb with XhoI-pMMBKn-for and SpeI-pMMBKn-rev. The *hph* resistance cassette was amplified using a lysate of a 5075 T101 mutant from the 5075 ordered library (42) as template and the primers SpeI-hph-for and XhoI-hph-rev. Inserts were digested with the restriction enzymes indicated by their primer names. Insert and vectors were ligated by T4 DNA Ligase (NEB) and transformed by electroporation into DH5α competent cells. Correct insert was confirmed by whole plasmid sequencing with Plasmidsaurus.

pBAD18kn-express was built by amplifying the *frt* flanked *kan* cassette from pKD4 with ClaI-kan-for and ClaI-kan-rev. pBAD18 vector and insert were digested with the restriction enzymes indicated by their primer names. Vector was treated with alkaline phosphatase. Insert and vectors were ligated by T4 DNA Ligase (NEB) and transformed by electroporation into DH5α competent cells. Correct insert was confirmed by whole plasmid sequencing with Plasmidsaurus.

pBaM1 was built by amplifying the backbone of pMMB67EHkan with primers PacI-pMMB-swap-for and PacI-pMMB-swap-rev. The insert *frt-kan-frt-araC*-pBAD promoter was amplified from pBAD18kn-express with primers PacI-pBAD-fr and PacI-pBAD-rv. Inserts were digested with the restriction enzymes indicated by their primer names. Insert and vectors were ligated by T4 DNA Ligase (NEB) and transformed by electroporation into DH5α competent cells. Correct insert was confirmed by whole plasmid sequencing with Plasmidsaurus.

pBaM3 was built by amplifying the *tetR* regulator and *tetR/tetA* promoter from p-dcas9-bacteria (73) with primers ClaI-ptet-for and EcoRI-ptet-rev. pBaM1 vector and insert were digested with the restriction enzymes indicated by primer names. Vector was treated with alkaline phosphatase. Insert and vectors were ligated by T4 DNA Ligase (NEB) and transformed by electroporation into DH5α competent cells. Correct insert was confirmed by whole plasmid sequencing with Plasmidsaurus.

Pseudomonas aeruginosa PA01 alleles of *lbcA* and *amiB*, *lbcA* and *oxa51*, *nlpD* and *amiB*, and *nlpD* and *oxa51* were codon optimized for expression in *E. coli* (GenScript). Gene synthesized products were designed to have an EcoRI cut site, AGGAGA ribosome binding site, putative activator (*lbcA* or *nlpD*), KpnI cut site, AGGAGA ribosome binding site, putative amidase (*amiB* or *oxa51*), and XbaI cut site. Gene synthesis was performed by GenScript in the pUC57mini plasmid.

Complementation and overexpression plasmids were built by digesting pMMB67EHtet with appropriate restriction enzymes (NEB) and treating digested plasmid with Antarctic Phosphatase (NEB). Inserts were digested with the restriction enzymes indicated by their primer names. Insert and vectors were ligated by T4 DNA Ligase (NEB) and transformed by electroporation into DH5α competent cells. Plasmids were screened by colony PCR with the primers ptac-seq and rrnB-T1-term-seq for the correct insert size and whole plasmid sequenced with Plasmidsaurus.

Whole-genome sequencing. Strains that were whole genome sequenced are indicated in **Data Set S1**. Whole-genome sequencing of mutants was performed by growing the strain overnight in 5 mL of LB. 1 mL of culture was pelleted at 13,000 x *g* for 1 min and frozen at -20 °C. Cell pellets were shipped to SeqCenter, LLC for gDNA extraction and whole genome sequencing. Reads were locally aligned, and variants mapped using CLC Genomics Workbench (Qiagen).

Microscopy. Overnight cultures were diluted into fresh 5 mL cultures of appropriate media at OD_{600} ~0.05. Strains were grown to OD_{600} ~0.5-0.7 and 1ul was spotted on VWR No. 1.5, 50X22mm rectangular micro cover glass (48393-195). Difco Minimal Agar Davis (254410) pads were placed on top of samples and imaged camera at 100x magnification on an inverted Nikon Eclipse TI2-E equipped with an Orca-Fusion Gen-III sCMOS camera and CFI60 Plan Apochromat Lambda Phase Contrast DM 100x Oil Immersion Objective Lens. NIS Elements software was used to acquire Z-stack images with a range of 1um, 7 steps per capture, 0.2 um per step. Three plains of each Z-stack were averaged with a Z-projection using ImageJ. Z-projections assisted in viewing of the highly kinked chains of *wthA* mutants which often extended slightly up and down along the Z-plane even with the flattening effects of agar pads. For consistency, all microscopy was performed and processed in the same manner.

Growth curves. Overnight cultures were diluted into fresh 5 mL of appropriate media at a starting OD_{600} of 0.05. Cultures were incubated at 37 °C until stationary phase was apparent, when a dip in OD_{600} indicated that lysis may occur the cultures were continued for 1-2 hours to see if this drop continued. At each timepoint, 200 μl of culture was transferred to wells in a 96-well flat-bottom polystyrene costar® microtiter plate (Corning) to measure OD_{600} on a Synergy H1 Hybrid reader with Gen5 software (BioTek®).

Overnight cultures for depletion of *wthA* contained 10 nM aTc. To assist in depletion of the tet-inducible *wthA* allele, cultures were diluted as described above into fresh 5mL of LB with

appropriate supplements. At the 2 hour time point, 50 μl of each culture was diluted again into a fresh 5mL of the same media to perform a single back-dilution.

Sensitivity to cold storage assessment. Strains were struck on two separate LB plates. After incubation at 37 °C one plate of each was stored at room temperature and one plate at 4 °C for 7-8 days. Single colonies from each storage condition were restruck on LB plates and incubated at 37 °C. The experiment was performed in triplicate for all strains.

MIC determination. Overnight cultures were grown in biological triplicate for each strain in 5 mL of LB with appropriate supplements. To assist in depletion of tet inducible strains, overnight cultures were grown with no aTc. Cotton-tipped applicator sticks were used to spread a lawn of each overnight on LB agar plates and the indicated E-test strip (Liofilchem®) was added to each lawn. Plates were incubated at 37 °C for ~16 hours and the MIC determined by where the lawn bisects the E-test strip.

Suppressor isolation. Overnight cultures of 19606 Δ*wthA* were grown in LB. 50 μl of each overnight was diluted in fresh 5 mL of LB with 5% glycerol and incubated at 37 °C for 24 hours. 50 μl of each 5% glycerol culture was diluted in fresh 5mL of LB with 10 % glycerol and incubated at 37 °C for 24 hours. 1 mL of cells was pelleted at max speed for 1 min for cultures with high optical density after growth in LB with 10% glycerol. The supernatant was removed, and pellets were whole genome sequenced as described above at SeqCenter, LLC.

PG amidase products release assay. The strain *E. coli* W3110 Δ*oppBCDF::frt* Δ*cadB::frt* was used for assays for release of PG amidase products (55, 56). The strain is missing both transporters for recycling of amidase products, but still has that transporter AmpG intact to recycle the products of endopeptidases and lytic transglycosylases. All 2-5 mL cultures for radioactive assays were grown in glass tubes and all 30 mL cultures were performed in 125 mL sterile disposable PETG plain bottom flasks with vented closures (Thermo Scientific). As described previously, ^{3}H Dap (American Radiolabeled Chemicals Inc., (DL+meso)-2,6-diaminopimelic acid [2,6-^{3}H], 60 Ci/mmol, 1 mCi/mL stock) was used to label the PG peptide in 2 mL overnight cultures of LB with 500 nCi/mL of ^{3}H-Dap and 5 μg/mL of tetracycline. 50 μl of overnight cultures was diluted into fresh 5 mL of LB with 500 nCi/mL of ^{3}H-Dap, 5 μg/mL of tetracycline, and the indicated concentrations of IPTG. Cultures were grown at 37 °C for 3-4 hours to OD_{600} ~1.0. The 5 mL cultures were transferred to 15 mL conical tubes and centrifuged at 5,000 x *g* for 5 min. Supernatants were discarded and cell pellets were resuspended in fresh 5 mL of LB with tetracycline and IPTG. The 5 mL resuspensions were diluted into total volume of 30 mL of fresh, pre-warmed LB with a final concentration of 30 μg/mL of cold mDap (2,6-diaminopimelic acid, Sigma) and tetracycline and IPTG. A 0 min time point was taken and strains were grown at 37 °C for a total of 2 hours to assess release during logarithmic growth. During growth, cultures were removed every 30 min and processed as follows: i) the OD_{600} was read in cuvettes, and ii) 500 μl of each sample was transferred to a 1.5 mL centrifuge tube and centrifuged at 17,000 x *g* for 2 min. Supernatants, containing ^{3}H-Dap that had been released from the cell, were carefully pipetted off and pellets, containing cellular ^{3}H-Dap that had been retained and/or recycled, were resuspended in 50 μl of PBS. 10 μl of the cellular resuspension was diluted into 5 mL of ScintiVerse™ BD cocktail (Fisher) in scintillation vials and vortexed. Liquid scintillation was counted by a Tri-Carb® 4910 TR liquid scintillation counter (PerkinElmer) with QuantaSmart™ program. The percent of tritium products released was calculated by percent of tritium lost comparing the 0 and 120 min time-points.

Bioinformatic analyses. A summary of the homolog search results is in in **Data Set S1**. All homologs were identified by blasting known genes from *E. coli* (for EnvC/NlpD/ActS), *A. baumannii* (for WthA), or *Caulobacter* (for DipM). Significant hits were all verified by blasting the hit back against these genomes to identify the gene it was most similar to, and by searching for literature that may have described an alternative function for the hit with PaperBlast (74). SignalP-5.0 (75)

was used to check localization of each allele. A phylogenic tree was generated using PhyloT v2 and the tree was visualized and annotated with iTOL (76).

Data availability

All data related to this paper are within the text, supplemental, or may be requested from the authors.

Acknowledgments

We gratefully acknowledge funding from the National Institutes of Health, grants AI176776, AI138576, and AI150098 (to M.S.T.); funding from the Army Research Office (ARO, http://www.arl.army.mil/) grant W911NF2010195 (to M.S.T.); and grant F32 GM137554 (to B.W.S.).

References

1. M. J. McConnell, L. Actis, J. Pachón, Acinetobacter baumannii: human infections, factors contributing to pathogenesis and animal models. *FEMS Microbiol Rev* **37**, 130–155 (2013).

2. A. Howard, M. O'Donoghue, A. Feeney, R. D. Sleator, Acinetobacter baumannii: an emerging opportunistic pathogen. *Virulence* **3**, 243–250 (2012).

3. L. Dijkshoorn, A. Nemec, H. Seifert, An increasing threat in hospitals: multidrug-resistant Acinetobacter baumannii. *Nat Rev Microbiol* **5**, 939–951 (2007).

4. Y. Funahara, H. Nikaido, Asymmetric localization of lipopolysaccharides on the outer membrane of Salmonella typhimurium. *J Bacteriol* **141**, 1463–1465 (1980).

5. Y. Kamio, H. Nikaido, Outer membrane of Salmonella typhimurium: accessibility of phospholipid head groups to phospholipase c and cyanogen bromide activated dextran in the external medium. *Biochemistry* **15**, 2561–2570 (1976).

6. E. Lundstedt, D. Kahne, N. Ruiz, Assembly and Maintenance of Lipids at the Bacterial Outer Membrane. *Chem Rev* (2020). https://doi.org/10.1021/acs.chemrev.0c00587.

7. H. Nikaido, Molecular basis of bacterial outer membrane permeability revisited. *Microbiol Mol Biol Rev* **67**, 593–656 (2003).

8. E. R. Rojas, *et al.*, The outer membrane is an essential load-bearing element in Gram-negative bacteria. *Nature* **559**, 617–621 (2018).

9. J. Berry, M. Rajaure, T. Pang, R. Young, The spanin complex is essential for lambda lysis. *J Bacteriol* **194**, 5667–5674 (2012).

10. M. Rajaure, J. Berry, R. Kongari, J. Cahill, R. Young, Membrane fusion during phage lysis. *Proc Natl Acad Sci U S A* **112**, 5497–5502 (2015).

11. B. W. Simpson, *et al.*, Acinetobacter baumannii Can Survive with an Outer Membrane Lacking Lipooligosaccharide Due to Structural Support from Elongasome Peptidoglycan Synthesis. *mBio* **12**, e0309921 (2021).

12. B. W. Simpson, M. S. Trent, Pushing the envelope: LPS modifications and their consequences. *Nat Rev Microbiol* **17**, 403–416 (2019).

13. R. L. Nation, T. Velkov, J. Li, Colistin and polymyxin B: peas in a pod, or chalk and cheese? *Clin Infect Dis* **59**, 88–94 (2014).

14. Z. Kassamali, J. C. Rotschafer, R. N. Jones, R. A. Prince, L. H. Danziger, Polymyxins: wisdom does not always come with age. *Clin Infect Dis* **57**, 877–883 (2013).

15. J. H. Moffatt, *et al.*, Colistin resistance in Acinetobacter baumannii is mediated by complete loss of lipopolysaccharide production. *Antimicrob Agents Chemother* **54**, 4971–4977 (2010).

16. J. M. Boll, *et al.*, A penicillin-binding protein inhibits selection of colistin-resistant, lipooligosaccharide-deficient Acinetobacter baumannii. *Proc Natl Acad Sci U S A* **113**, E6228–E6237 (2016).

17. L. Steeghs, *et al.*, Meningitis bacterium is viable without endotoxin. *Nature* **392**, 449–450 (1998).

18. D. Peng, W. Hong, B. P. Choudhury, R. W. Carlson, X.-X. Gu, Moraxella catarrhalis bacterium without endotoxin, a potential vaccine candidate. *Infect Immun* **73**, 7569–7577 (2005).

19. J. J. Zik, *et al.*, Caulobacter lipid A is conditionally dispensable in the absence of fur and in the presence of anionic sphingolipids. *Cell Rep* **39**, 110888 (2022).

20. A. Beceiro, *et al.*, Biological cost of different mechanisms of colistin resistance and their impact on virulence in Acinetobacter baumannii. *Antimicrob Agents Chemother* **58**, 518–526 (2014).

21. M. J. Powers, M. S. Trent, Phospholipid retention in the absence of asymmetry strengthens the outer membrane permeability barrier to last-resort antibiotics. *Proc Natl Acad Sci U S A* **115**, E8518–E8527 (2018).

22. K. N. Kang, *et al.*, Septal Class A Penicillin-Binding Protein Activity and ld-Transpeptidases Mediate Selection of Colistin-Resistant Lipooligosaccharide-Deficient Acinetobacter baumannii. *mBio* **12** (2021).

23. P. D. A. Rohs, T. G. Bernhardt, Growth and Division of the Peptidoglycan Matrix. *Annu Rev Microbiol* **75**, 315–336 (2021).

24. S. Kumar, A. Mollo, D. Kahne, N. Ruiz, The Bacterial Cell Wall: From Lipid II Flipping to Polymerization. *Chem Rev* **122**, 8884–8910 (2022).

25. M.-J. Tsang, A. A. Yakhnina, T. G. Bernhardt, NlpD links cell wall remodeling and outer membrane invagination during cytokinesis in Escherichia coli. *PLoS Genet* **13**, e1006888 (2017).

26. M. A. Gerding, Y. Ogata, N. D. Pecora, H. Niki, P. A. J. de Boer, The trans-envelope Tol-Pal complex is part of the cell division machinery and required for proper outer-membrane invagination during cell constriction in E. coli. *Mol Microbiol* **63**, 1008–1025 (2007).

27. R. Shrivastava, X. Jiang, S.-S. Chng, Outer membrane lipid homeostasis via retrograde phospholipid transport in Escherichia coli. *Mol Microbiol* **106**, 395–408 (2017).

28. T. Uehara, K. R. Parzych, T. Dinh, T. G. Bernhardt, Daughter cell separation is controlled by cytokinetic ring-activated cell wall hydrolysis. *EMBO J* **29**, 1412–1422 (2010).

29. T. Uehara, T. Dinh, T. G. Bernhardt, LytM-domain factors are required for daughter cell separation and rapid ampicillin-induced lysis in Escherichia coli. *J Bacteriol* **191**, 5094–5107 (2009).

30. C. K. Gurnani Serrano, *et al.*, ActS activates peptidoglycan amidases during outer membrane stress in Escherichia coli. *Mol Microbiol* **116**, 329–342 (2021).

31. P. K. Chodisetti, R. Bahadur, R. N. Amrutha, M. Reddy, A LytM-Domain Factor, ActS, Functions in Two Distinctive Peptidoglycan Hydrolytic Pathways in E. coli. *Front Microbiol* **13**, 913949 (2022).

32. C. R. Mahone, E. D. Goley, Bacterial cell division at a glance. *J Cell Sci* **133** (2020).

33. R. McQuillen, J. Xiao, Insights into the Structure, Function, and Dynamics of the Bacterial Cytokinetic FtsZ-Ring. *Annu Rev Biophys* **49**, 309–341 (2020).

34. J. Cook, *et al.*, Insights into bacterial cell division from a structure of EnvC bound to the FtsX periplasmic domain. *Proc Natl Acad Sci U S A* **117**, 28355–28365 (2020).

35. J. Cook, *et al.*, Activator-induced conformational changes regulate division-associated peptidoglycan amidases. *Proc Natl Acad Sci U S A* **120**, e2302580120 (2023).

36. S. Du, S. Pichoff, J. Lutkenhaus, Roles of ATP Hydrolysis by FtsEX and Interaction with FtsA in Regulation of Septal Peptidoglycan Synthesis and Hydrolysis. *mBio* **11** (2020).

37. A. Yahashiri, M. A. Jorgenson, D. S. Weiss, Bacterial SPOR domains are recruited to septal peptidoglycan by binding to glycan strands that lack stem peptides. *Proc Natl Acad Sci U S A* **112**, 11347–11352 (2015).

38. M. A. Gerding, *et al.*, Self-enhanced accumulation of FtsN at Division Sites and Roles for Other Proteins with a SPOR domain (DamX, DedD, and RlpA) in Escherichia coli cell constriction. *J Bacteriol* **191**, 7383–7401 (2009).

39. B. Liu, L. Persons, L. Lee, P. A. J. de Boer, Roles for both FtsA and the FtsBLQ subcomplex in FtsN-stimulated cell constriction in Escherichia coli. *Mol Microbiol* **95**, 945–970 (2015).

40. M.-J. Tsang, T. G. Bernhardt, A role for the FtsQLB complex in cytokinetic ring activation revealed by an ftsL allele that accelerates division. *Mol Microbiol* **95**, 925–944 (2015).

41. K.-T. Park, S. Pichoff, S. Du, J. Lutkenhaus, FtsA acts through FtsW to promote cell wall synthesis during cell division in Escherichia coli. *Proc Natl Acad Sci U S A* **118** (2021).

42. L. A. Gallagher, *et al.*, Resources for Genetic and Genomic Analysis of Emerging Pathogen Acinetobacter baumannii. *J Bacteriol* **197**, 2027–2035 (2015).

43. N. Wang, E. A. Ozer, M. J. Mandel, A. R. Hauser, Genome-wide identification of Acinetobacter baumannii genes necessary for persistence in the lung. *mBio* **5**, e01163-01114 (2014).

44. T. Do, *et al.*, Staphylococcus aureus cell growth and division are regulated by an amidase that trims peptides from uncrosslinked peptidoglycan. *Nat Microbiol* **5**, 291–303 (2020).

45. J. E. Page, M. A. Skiba, T. Do, A. C. Kruse, S. Walker, Metal cofactor stabilization by a partner protein is a widespread strategy employed for amidase activation. *Proc Natl Acad Sci U S A* **119**, e2201141119 (2022).

46. J. M. Colquhoun, *et al.*, OXA-23 β-Lactamase Overexpression in Acinetobacter baumannii Drives Physiological Changes Resulting in New Genetic Vulnerabilities. *mBio* **12**, e0313721 (2021).

47. D. Srivastava, *et al.*, A Proteolytic Complex Targets Multiple Cell Wall Hydrolases in Pseudomonas aeruginosa. *mBio* **9** (2018).

48. D. Chakraborty, A. J. Darwin, Direct and Indirect Interactions Promote Complexes of the Lipoprotein LbcA, the CtpA Protease and Its Substrates, and Other Cell Wall Proteins in Pseudomonas aeruginosa. *J Bacteriol* **203**, e0039321 (2021).

49. C. Heidrich, A. Ursinus, J. Berger, H. Schwarz, J.-V. Höltje, Effects of multiple deletions of murein hydrolases on viability, septum cleavage, and sensitivity to large toxic molecules in Escherichia coli. *J Bacteriol* **184**, 6093–6099 (2002).

50. A. Tomasz, A. Albino, E. Zanati, Multiple antibiotic resistance in a bacterium with suppressed autolytic system. *Nature* **227**, 138–140 (1970).

51. A. Tomasz, S. Waks, Mechanism of action of penicillin: triggering of the pneumococcal autolytic enzyme by inhibitors of cell wall synthesis. *Proc Natl Acad Sci U S A* **72**, 4162–4166 (1975).

52. H. S. Chung, *et al.*, Rapid beta-lactam-induced lysis requires successful assembly of the cell division machinery. *Proc Natl Acad Sci U S A* **106**, 21872–21877 (2009).

53. A. A. Yakhnina, H. R. McManus, T. G. Bernhardt, The cell wall amidase AmiB is essential for Pseudomonas aeruginosa cell division, drug resistance and viability. *Mol Microbiol* **97**, 957–973 (2015).

54. C. Fröhlich, J. Z. Chen, S. Gholipour, A. N. Erdogan, N. Tokuriki, Evolution of β-lactamases and enzyme promiscuity. *Protein Eng Des Sel* **34**, gzab013 (2021).

55. B. W. Simpson, M. C. Gilmore, A. B. McLean, F. Cava, M. S. Trent, Escherichia coli utilizes multiple peptidoglycan recycling permeases with distinct strategies of recycling. *Proceedings of the National Academy of Sciences of the United States of America* **120**, e2308940120 (2023).

56. B. W. Simpson, M. C. Gilmore, A. B. McLean, F. Cava, M. S. Trent, Escherichia coli CadB is capable of promiscuously transporting muropeptides and contributing to peptidoglycan recycling. *J Bacteriol* **206**, e0036923 (2024).

57. O. Irazoki, S. B. Hernandez, F. Cava, Peptidoglycan Muropeptides: Release, Perception, and Functions as Signaling Molecules. *Front Microbiol* **10**, 500 (2019).

58. J. T. Park, D. Raychaudhuri, H. Li, S. Normark, D. Mengin-Lecreulx, MppA, a periplasmic binding protein essential for import of the bacterial cell wall peptide L-alanyl-gamma-D-glutamyl-meso-diaminopimelate. *J Bacteriol* **180**, 1215–1223 (1998).

59. Q. Cheng, J. T. Park, Substrate specificity of the AmpG permease required for recycling of cell wall anhydro-muropeptides. *J Bacteriol* **184**, 6434–6436 (2002).

60. A. Maqbool, *et al.*, Compensating stereochemical changes allow murein tripeptide to be accommodated in a conventional peptide-binding protein. *J Biol Chem* **286**, 31512–31521 (2011).

61. A. Möll, S. Schlimpert, A. Briegel, G. J. Jensen, M. Thanbichler, DipM, a new factor required for peptidoglycan remodelling during cell division in Caulobacter crescentus. *Mol Microbiol* **77**, 90–107 (2010).

62. D. Szklarczyk, *et al.*, The STRING database in 2023: protein-protein association networks and functional enrichment analyses for any sequenced genome of interest. *Nucleic Acids Res* **51**, D638–D646 (2023).

63. F. Madeira, *et al.*, The EMBL-EBI search and sequence analysis tools APIs in 2019. *Nucleic Acids Res* **47**, W636–W641 (2019).

64. E. Geisinger, *et al.*, Antibiotic susceptibility signatures identify potential antimicrobial targets in the Acinetobacter baumannii cell envelope. *Nat Commun* **11**, 4522 (2020).

65. J. Bai, *et al.*, Essential Gene Analysis in Acinetobacter baumannii by High-Density Transposon Mutagenesis and CRISPR Interference. *J Bacteriol* **203**, e0056520 (2021).

66. R. D. Ward, *et al.*, Essential gene knockdowns reveal genetic vulnerabilities and antibiotic sensitivities in Acinetobacter baumannii. *mBio* **15**, e0205123 (2024).

67. H.-C. Hsu, M. Wang, A. Kovach, A. J. Darwin, H. Li, Pseudomonas aeruginosa C-Terminal Processing Protease CtpA Assembles into a Hexameric Structure That Requires Activation by a Spiral-Shaped Lipoprotein-Binding Partner. *mBio* **13**, e0368021 (2022).

68. H.-C. Hsu, M. Wang, A. Kovach, A. J. Darwin, H. Li, P. aeruginosa CtpA protease adopts a novel activation mechanism to initiate the proteolytic process. *EMBO J* **43**, 1634–1652 (2024).

69. P. Lestrate, *et al.*, Attenuated signature-tagged mutagenesis mutants of Brucella melitensis identified during the acute phase of infection in mice. *Infect Immun* **71**, 7053–7060 (2003).

70. J. Herrou, *et al.*, Brucella Periplasmic Protein EipB Is a Molecular Determinant of Cell Envelope Integrity and Virulence. *J Bacteriol* **201** (2019).

71. K. D. Neudorf, E. M. Vanderlinde, D. D. Tambalo, C. K. Yost, A previously uncharacterized tetratricopeptide-repeat-containing protein is involved in cell envelope function in Rhizobium leguminosarum. *Microbiology (Reading)* **161**, 148–157 (2015).

72. A. T. Tucker, *et al.*, Defining gene-phenotype relationships in Acinetobacter baumannii through one-step chromosomal gene inactivation. *mBio* **5**, e01313-01314 (2014).

73. L. S. Qi, *et al.*, Repurposing CRISPR as an RNA-guided platform for sequence-specific control of gene expression. *Cell* **152**, 1173–1183 (2013).

74. M. N. Price, A. P. Arkin, PaperBLAST: Text Mining Papers for Information about Homologs. *mSystems* **2** (2017).

75. J. J. Almagro Armenteros, *et al.*, SignalP 5.0 improves signal peptide predictions using deep neural networks. *Nat Biotechnol* **37**, 420–423 (2019).

76. I. Letunic, P. Bork, Interactive Tree Of Life (iTOL) v5: an online tool for phylogenetic tree display and annotation. *Nucleic Acids Res* **49**, W293–W296 (2021).

Main Figure Legends

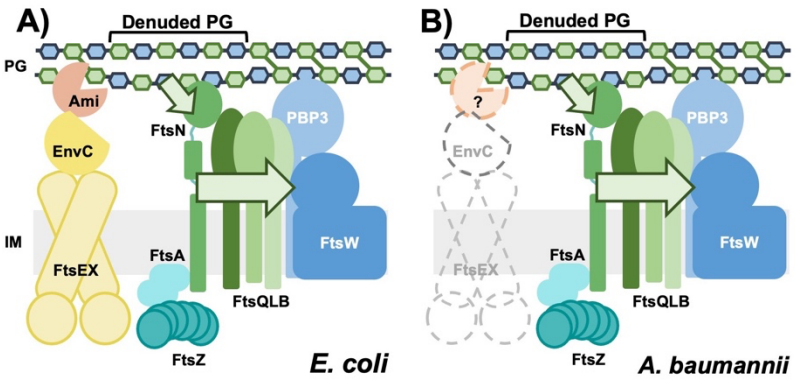

Figure 1. *A. baumannii* is missing homologs of key components involved in cell division. A) In *E. coli*, amidases (AmiA, AmiB, or AmiC) that cleave out the peptidoglycan (PG) peptides are highly regulated. During cell division, ATP hydrolysis by FtsEX causes a conformational change in EnvC releasing a self-inhibiting helix. EnvC then activates amidases, AmiB and AmiA, which cleave PG and leaves sugar chains "denuded" of crosslinked peptides. Denuded PG is recognized by the SPOR domain of FtsN. FtsN then signals to activate both PBP3 (divisome transpeptidase) through FtsQBL and FtsW (divisome glycosyltransferase) through FtsA. FtsN activation of FtsW/PBP3 serves as a self-enhancing loop of increased synthesis and remodeling of PG to drive division completion. B) *A. baumannii* is missing homologs of EnvC, FtsEX, and amidases, but still contains an essential FtsN homolog suggesting that it utilizes divergent amidases and activators to stimulate cell division.

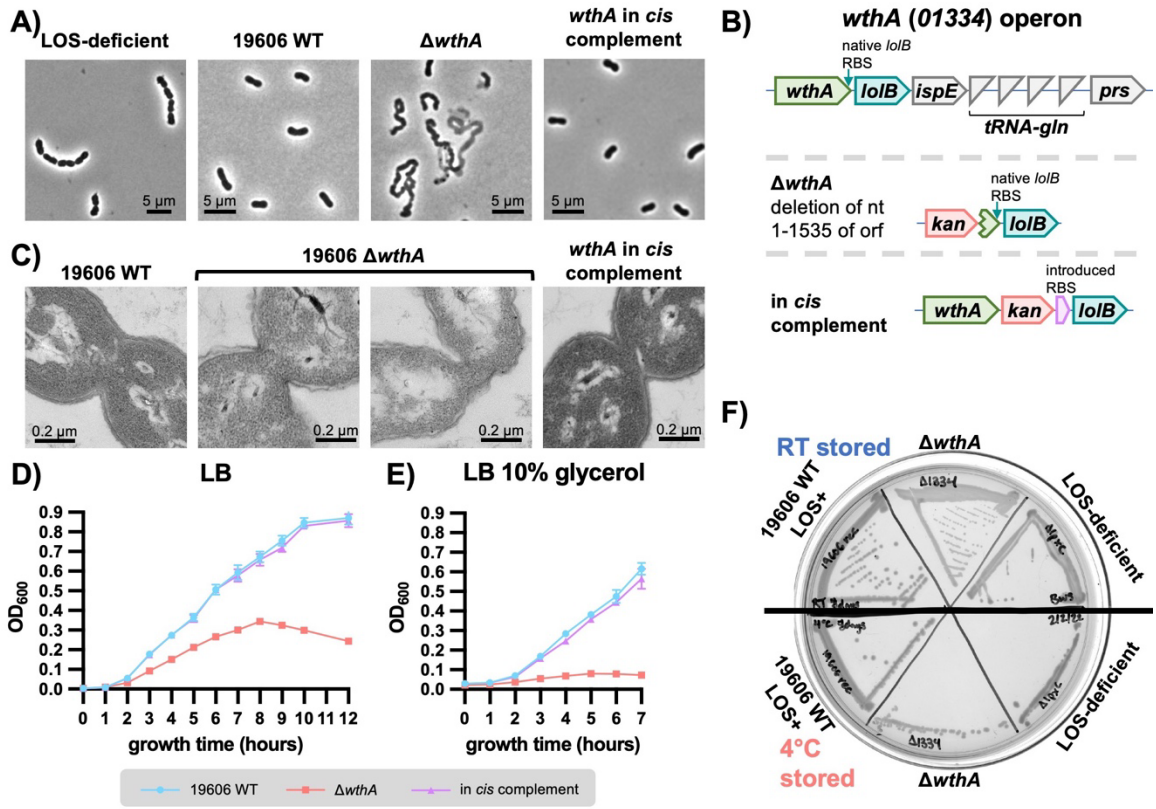

Figure 2. WthA (HMPREF0010_01334) impacts cell division and does not function in LOS-deficient *A. baumannii*. A) Phase contrast microscopy of LOS-deficient and *wthA* mutants, representative of biological triplicate. B) *wthA* operon structure and description of *wthA* mutant alleles. C) Transmission electron microscopy focusing on division sites of *wthA* mutants. D-E) Biological triplicate growth curves of *wthA* mutants in LB (D) or LB with 10% glycerol (E). Error bars are not shown when smaller than the size of the symbol. F) Growth of *wthA* and LOS-deficient mutants at 37 °C inoculated from colonies previously stored for 7-8 days at either room temperature (RT) or 4°C, representative of biological triplicate.

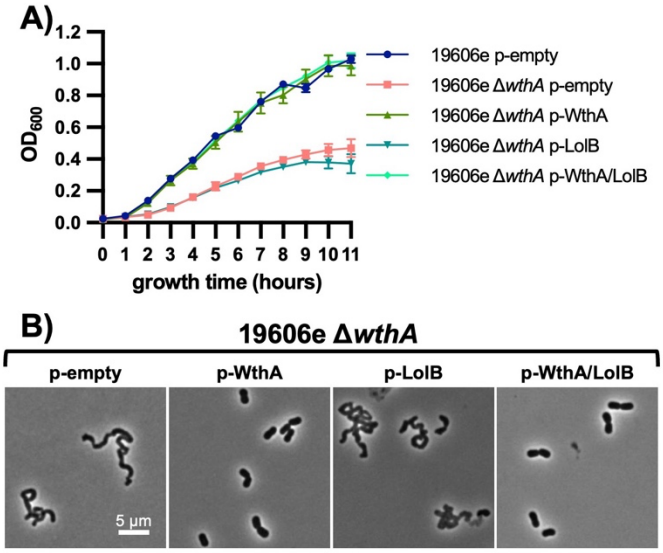

Figure 3. Defects from deletion of *wthA* are not due to polar effects on *lolB*. A) Biological triplicate growth curves in LB of the 19606e Δ*wthA* mutant with different plasmids to assess for complementation. Error bars are not shown when smaller than the size of the symbol. B) Representative phase contrast microscopy of biological triplicates of the indicated strains. Scale bar is the same for all microscopy images. (A-B) IPTG was used at a final concentration of 25 μM.

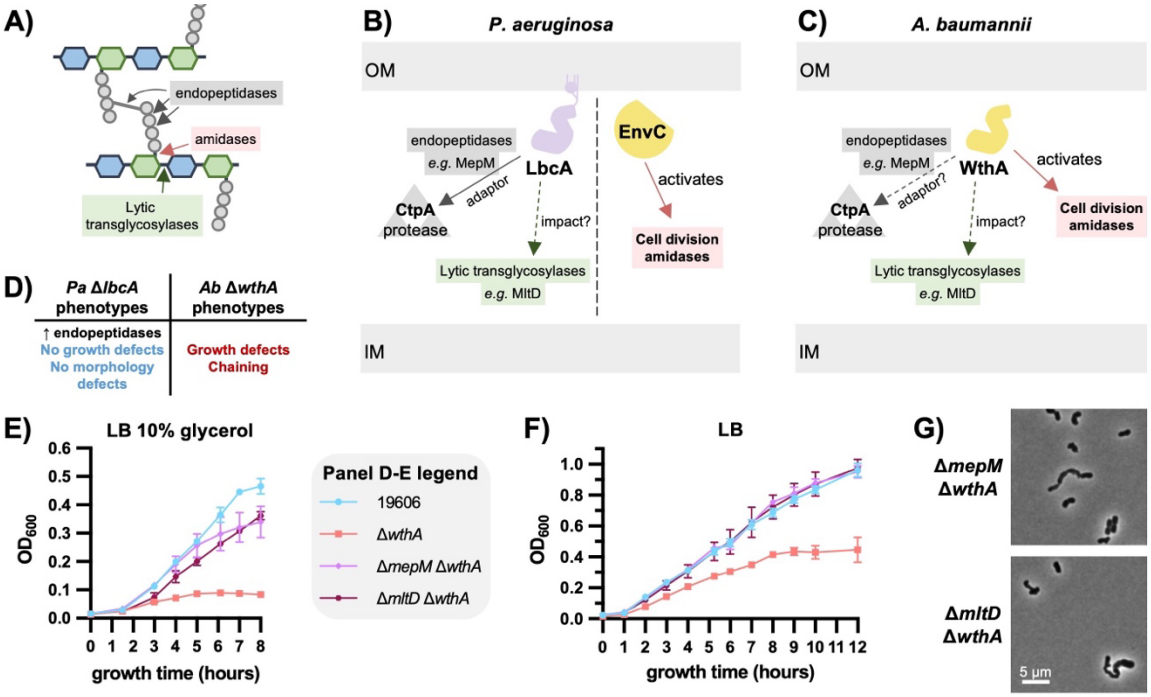

Figure 4. Suppressors that disrupt MepM and MltD rescue growth, but do not repair cell division defects. A) Cartoon depiction of the locations that different classes of PG turnover enzymes cleave PG. B) Regulation of PG turnover enzymes by LbcA (OM anchored homolog of WthA) and EnvC in *P. aeruginosa*. C) Possible role of WthA in regulating PG turnover enzymes based on homology to LbcA and observed cell division defect. D) Phenotypes observed for Δ*lbcA* and Δ*wthA* mutants. E-F) Biological triplicate growth curves of *wthA* suppressors grown in LB with 10% glycerol (E) and LB (F). Error bars are not shown when smaller than the size of the symbol. G) Phase contrast microscopy of *wthA* suppressors, representative of biological triplicates.

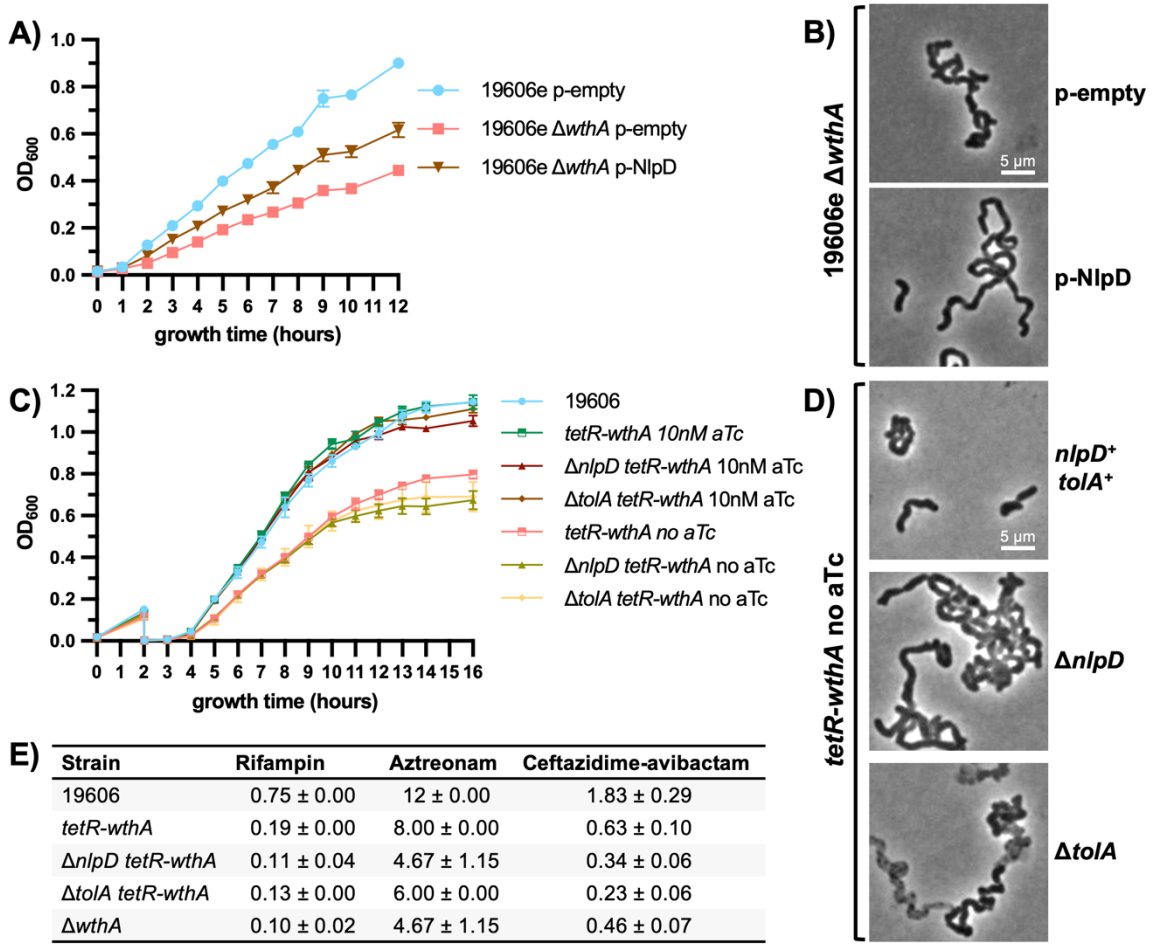

E)

Strain	Rifampin	Aztreonam	Ceftazidime-avibactam
19606	0.75 ± 0.00	12 ± 0.00	1.83 ± 0.29
tetR-wthA	0.19 ± 0.00	8.00 ± 0.00	0.63 ± 0.10
Δ*nlpD tetR-wthA*	0.11 ± 0.04	4.67 ± 1.15	0.34 ± 0.06
Δ*tolA tetR-wthA*	0.13 ± 0.00	6.00 ± 0.00	0.23 ± 0.06
Δ*wthA*	0.10 ± 0.02	4.67 ± 1.15	0.46 ± 0.07

Figure 5. WthA and NlpD are redundant, but not equivalent. A-B) Biological triplicate growth curve (A) and representative microscopy (B) of 19606e Δ*wthA* with or without NlpD overexpression. LB was supplemented with 10 µM IPTG. C) Biological triplicate growth curves in LB with either 10 nM aTc or no inducer. A single back-dilution was used to assist depletion of the aTc-regulated *wthA* allele. Error bars are not shown on growth curves when smaller than the size of the symbol. D) Phase contrast microscopy of *wthA* depletion strains grown in LB with no inducer. E) Minimal inhibitory concentrations of select antibiotics for *wthA* depletions strains grown without aTc inducer. Average and standard deviation of biological triplicates are shown.

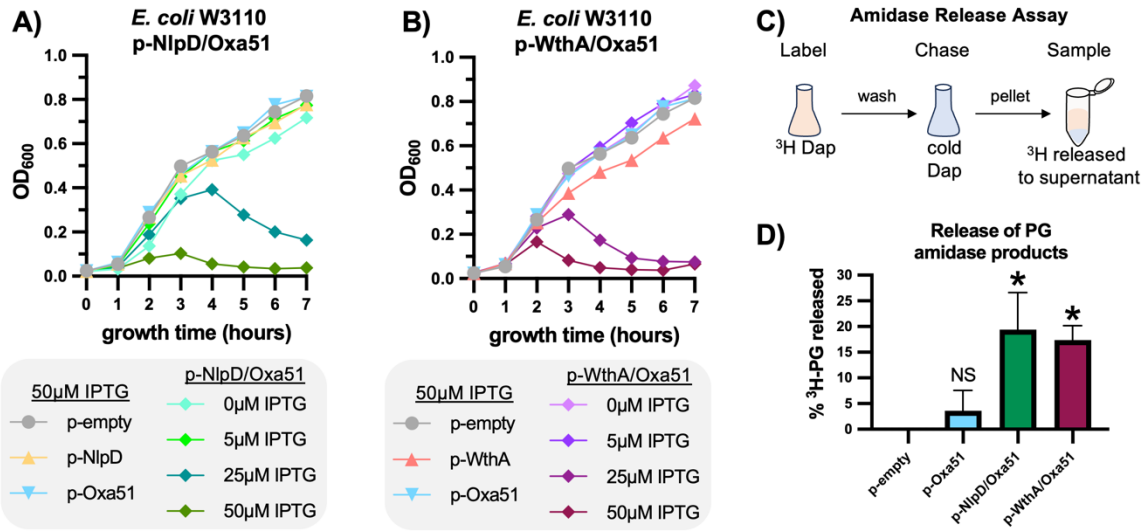

Figure 6. *A. baumannii* WthA and NlpD stimulate toxic amidase activity when co-expressed with the *β*-lactamase Oxa51. A-B) Growth curves of *A. baumannii* expressing only Oxa51, a *β*-lactamase proposed to produce amidase products, or in combination with putative amidase activators, NlpD(A) or WthA(B). Growth curves are representative of biological triplicates, grown in LB, and contained the indicated concentrations of IPTG. C) Schematic description of an amidase release assay using the *E. coli* W3110 Δ*opp* Δ*cadB* strain that specifically releases amidase freed PG peptides to the supernatant but recycles all other PG turnover products. Briefly, PG cell wall peptides were labeled with ^{3}H Dap, excess label was washed away, and loss of ^{3}H amidase products was monitored with sub-toxic expression of Oxa51 or Oxa51 combined with NlpD or WthA. D) Loss of ^{3}H amidase products during sub-toxic expression Oxa51 alone (10 μM IPTG), NlpD and Oxa51 (10 μM IPTG), or WthA and Oxa51 (5 μM IPTG). Empty plasmid (10 μM IPTG) was used as a control. Error bars show standard deviation of biological triplicate experiments. Significance was calculated by T-test. NS indicates not significant. * indicates $p<0.05$. Sub-toxic levels of expression was determined in **Fig. S4C-D**.

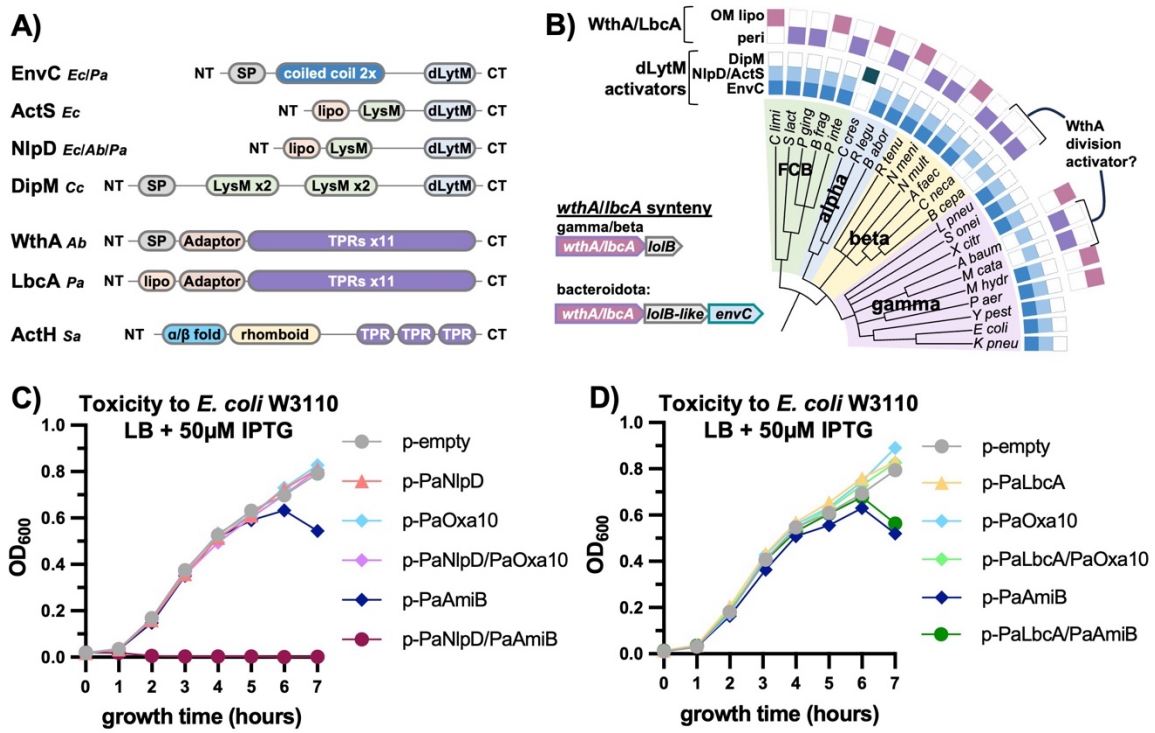

Figure 7. WthA/LbcA are a widely conserved family with distinct mechanisms of impacting PG turnover enzymes. A) Domains of protein families implicated in activating cell division amidases. dLytM indicates a degenerate peptidase domain that is missing critical catalytic residues. EnvC, NlpD, ActS, and DipM utilize dLytM domains to activate PG amidases. ActH and likely WthA utilize TPR (Tetratricopeptide repeat) domains to activate PG amidases. SP indicates signal peptide for periplasmic proteins. Lipo indicates lipoprotein signal peptides for OM anchored lipoproteins. B) Conservation of dLytM and WthA/LbcA homologs identified in proteobacteria (alpha, beta, and gamma subgroups) and FCB (Fibrobacterota, Chlorobiota, and Bacteroidota) phyla with identified synteny in different phyla. *lolB-like* genes indicated in synteny encode unknown function OM lipoproteins that String suggested were *lolB* homologs. For WthA/LbcA homologs, OM lipo indicates they are expected to encode an OM anchored lipoprotein. Peri indicates WthA/LbcA homologs that are expected to be soluble and periplasmic. (D-E) Growth curves of *E. coli* W3110 expressing the *P. aeruginosa* amidase, *Pa*AmiB, or the *β*-lactamase *Pa*Oxa10, alone or in combination with *P. aeruginosa Pa*NlpD (C) or *Pa*LbcA (D). Growth curves are representative of biological triplicates, grown in LB with 50 μM IPTG.

Supplemental Figure Legends

A)

Gene	Predicted function	LOS+ *v* LOS– FC	*p* value
**wthA*	periplasmic, TPR domains	11.71	0
nlpD	LysM-domain OM lipoprotein	-15.8	9.30E-90
yraP	division associated OM lipoprotein	-16.4	2.13E-33
pal	Pal, Tol-pal system	-42.2	0
tolB	TolB, Tol-pal system	-65.3	3.27E-99
tolA	TolA, Tol-pal system	-61.8	0
tolR	TolR, Tol-pal system	-49.4	2.66E-06
tolQ	TolQ, Tol-pal system	-56.6	1.22E-37

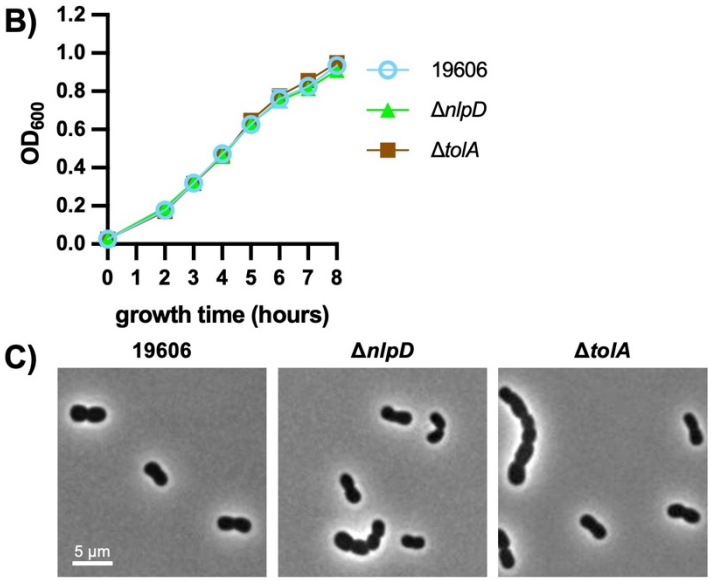

Fig S1. Phenotypes of *A. baumannii nlpD* and *tolA* mutants. A) NlpD, Tol-Pal, and YraP become critical for fitness in an LOS-deficient strain. *wthA* is easy to disrupt in LOS-deficient cells, perhaps because it does not function in the absence of LOS. B) Biological triplicate growth curves comparing growth of *A. baumannii* 19606 wild-type to growth of *nlpD* and *tolA* mutants. Error bars are not shown when smaller than the size of the symbol. C) Phase contrast microscopy of *nlpD* and *tolA* mutants, representative of biological triplicate.

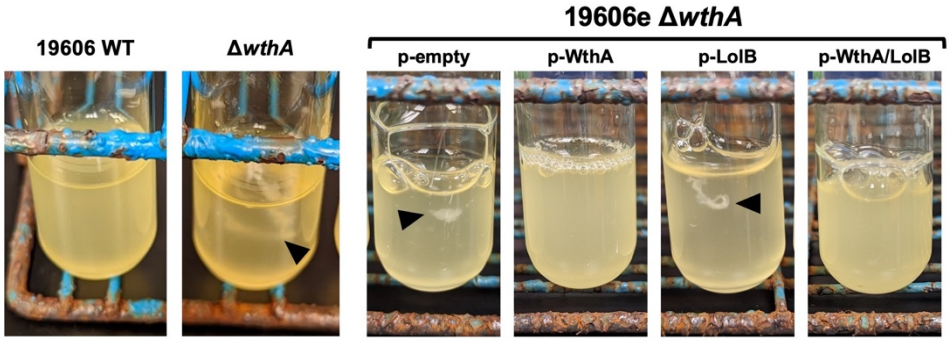

Figure S2. Cellular debris in overnights cultures of *wthA* mutants grown in LB. Clumped debris material is indicated with black arrow-heads and is accompanied by low density of overnight cultures. All images are representative of growth trends observed in at least biological triplicate. 19606e, electrocompetent, background is described in **Fig. S3**.

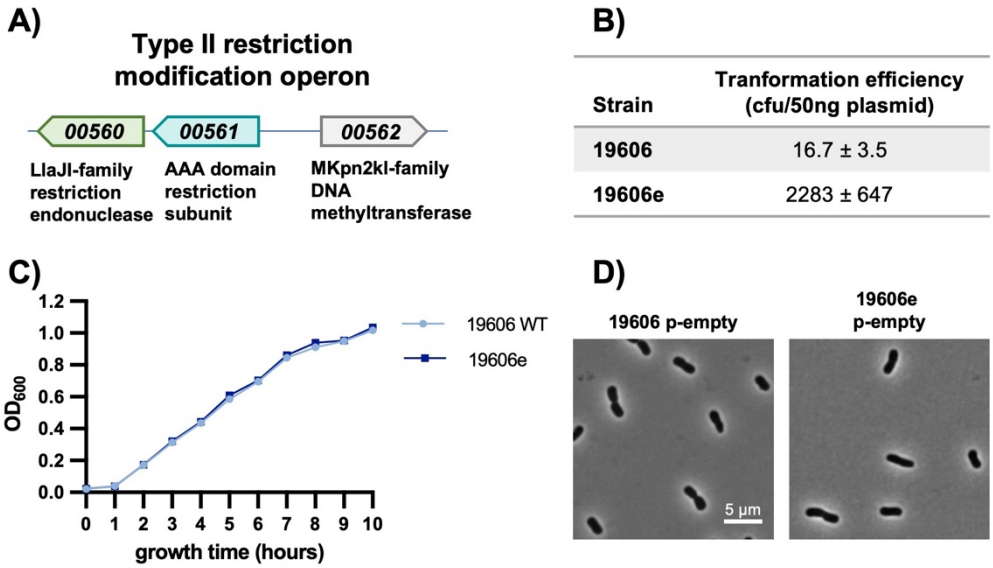

Figure S3. Generation of an electrocompetent strain of *A. baumannii* 19606 by deletion of the restriction endonuclease locus HMPREF0010_00560-00561. A) Operon structure of the HMPREF0010_00560-HMPREF0010_00562 restriction/modification system. B) Transformation efficiency of 19606 and the electrocompetent 19606e (Δ00560-00561) strains, average and standard deviation of biological triplicates. C) Growth curves of 19606 and 19606e strains in biological triplicate. Error bars are not shown when smaller than the size of the symbol. D) Phase contrast microscopy of 19606 and 19606e strains, representative of biological triplicates.

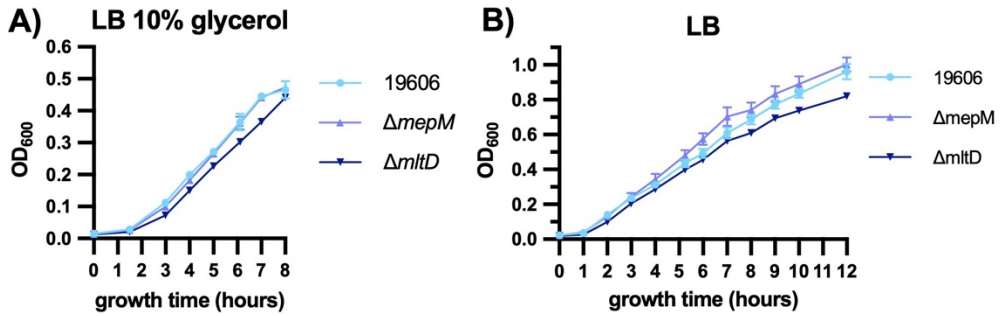

Figure S4. Effects of disrupting MepM and MltD in *A. baumannii*. A-B) Growth curves in LB (A) and LB + 10% glycerol (B) of *mepM* and *mltD* mutants. Data is from biological triplicate and error bars are not shown when smaller than the size of the symbol.

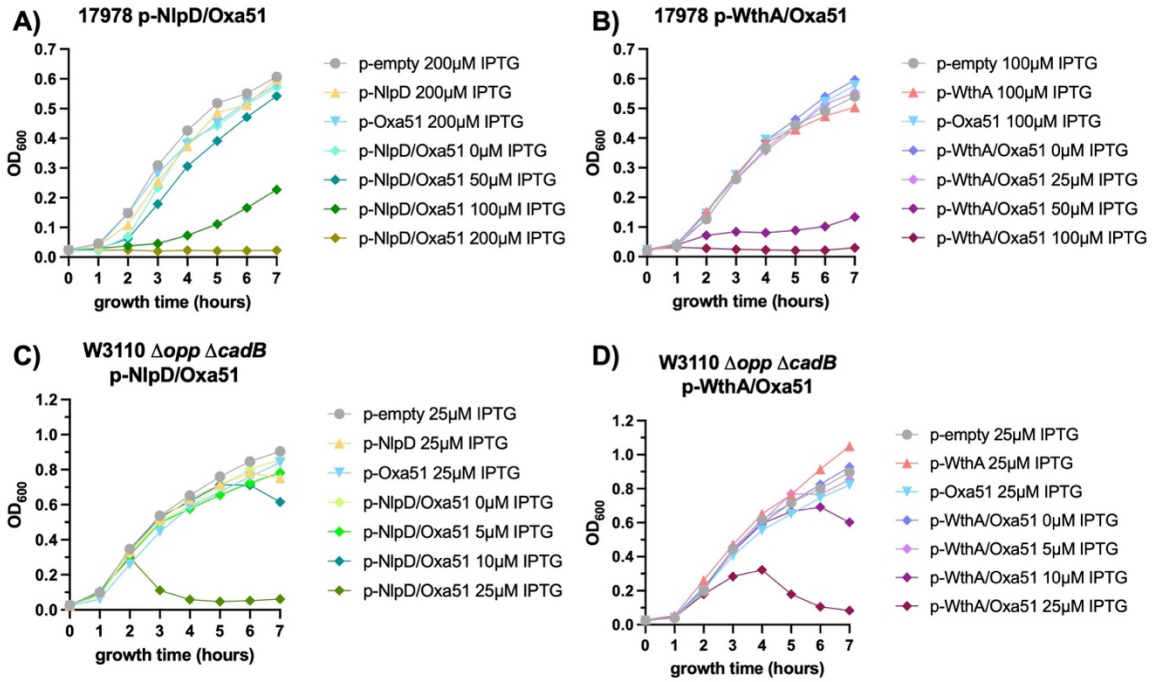

Figure S5. WthA and NlpD coexpression with the *β*-lactamase Oxa51. A-D) Growth curves of single or coexpressions of Oxa51 and putative amidase activators NlpD (A,C) or WthA (B,D) expressed in *A. baumannii* ATCC 17978 (A-B) or *E. coli* W3110 Δ*opp* Δ*cadB* (C-D). All growth curves are representatives of biological triplicates grown in LB and contained the indicated concentrations of IPTG.

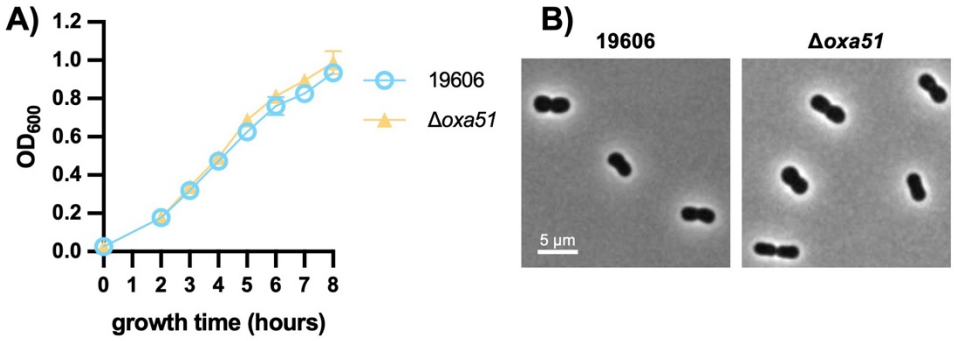

Figure S6. Loss of Oxa51 has no major impact on cell division. A) Growth curves comparing growth of *A. baumannii* 19606 wild-type to growth of an *oxa51* mutant. Data is from biological triplicate and error bars are not shown when smaller than the size of the symbol. B) Representative Phase contrast microscopy of an *oxa51* mutant, representative of biological triplicate.

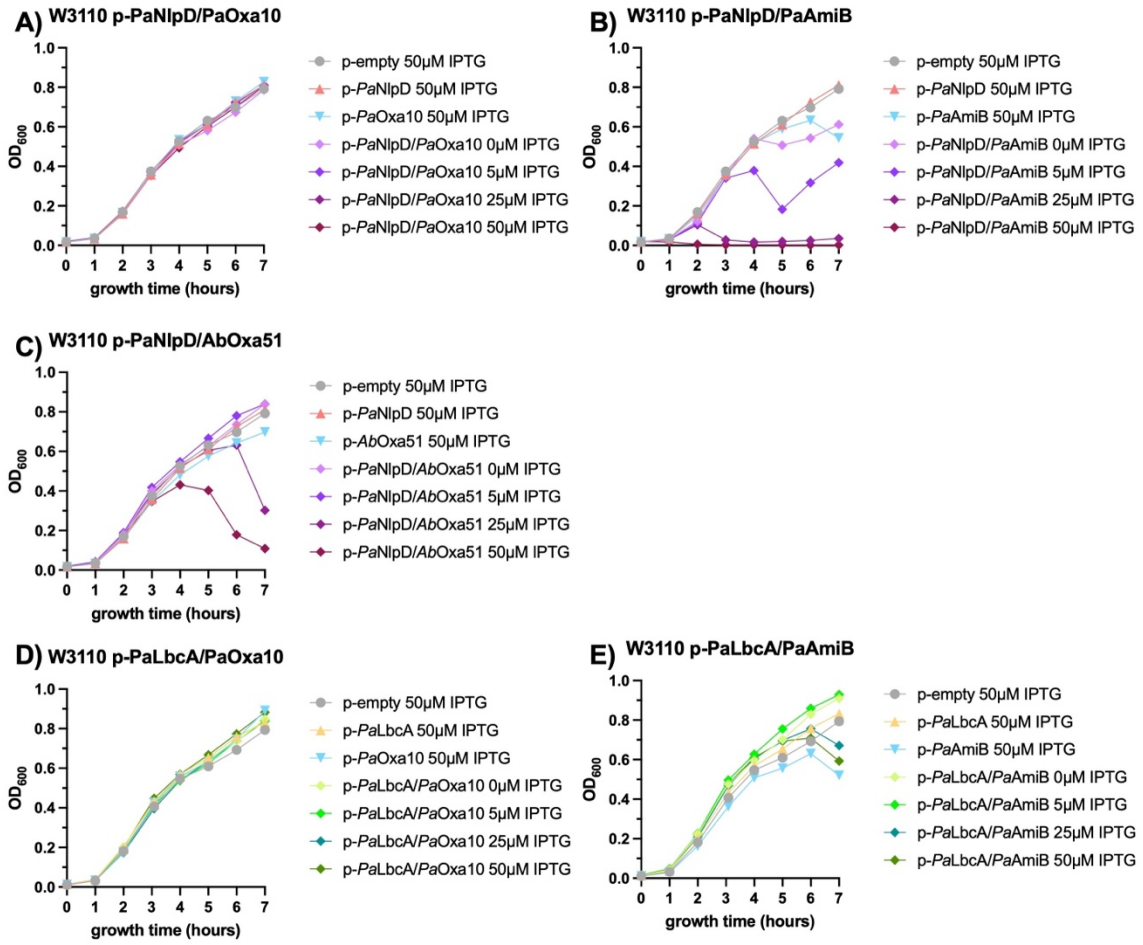

Figure S7. Toxicity screen to test *P. aeruginosa* homologs for amidase activation. A-E) Growth curves of *E. coli* W3110 expressing plasmids with possible amidases, *Pa*Oxa10 (A,D), *Pa*AmiB (B,E), and *Ab*Oxa51 (C) alone or in combination with possible amidase activators *Pa*NlpD (A-C) or *Pa*LbcA (D-E). All growth curves are representatives of biological triplicates, grown in LB, and contained the indicated concentrations of IPTG.

Table S1. Antibiotic sensitivity profile of *wthA* mutants indicates low PBP activity and uncrosslinked D-ala-D-ala.

Antibiotic	19606 MIC (Avg ± SD)	Δ*wthA* MIC (Avg ± SD)	Fold change	Target	Interpretation
Rifampicin	0.75 ± 0.00	0.104 ± 0.018	-7.2	RNA pol/ hydrophobic	OM disruption
Fosfomycin	85.3 ± 18.5	69.3 ± 24.4	-1.2	Lipid II synthesis	no impact
Vancomycin	74.7 ± 18.5	>256	>3.4	D-ala-D-ala	Uncrosslinked D-ala-D-ala
Ceftazidime-avibactam	1.83 ± 0.29	0.46 ± 0.07	-4.0	PG transpeptidases (PBP2/3/1A/1B)	decreased crosslinks
Aztreonam	12.0 ± 0.0	4.67 ± 1.15	-2.6	PBP3	cell division defect
Bacitracin	42.7 ± 9.2	32 ± 13.9	-1.3	UndP	no impact